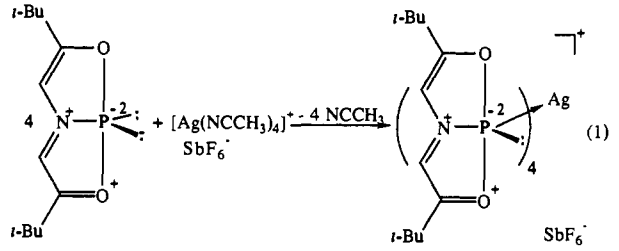

10-P-3 ADPO $[(ADPO)_4Ag]^+SbF_6^-$

The solid-state structure[13] of $[(ADPO)_4Ag]^+$ is illustrated in Figure 1. Silver (with an unusual square-planar geometry for an 18e, silver cation) is located on a 4-fold symmetry axis. This may be due to the unique steric requirement of accommodating 4 ADPO units, with each having ψ-tbp phosphorus centers. The Ag-P distance of 261.2 (1) pm is slightly shorter than the Ag-P distances seen for tetrahedral $Ag(PPh_3)_4^+$ (range 261.5→274.6 pm).[14-16] The ADPO ligand is essentially planar (largest deviation is 6.2 pm for one of the *t*-Bu bearing carbons) and has very similar structural parameters to those of uncomplexed 10-P-3 ADPO[5,17] (Table I). The N-P-Ag angle of 113.3 (1)° clearly indicates the stereochemical activity of a lone pair of phosphorus.

The multinuclear NMR and elemental analysis data are consistent with the above structure. Lability of the ADPO ligands in $(ADPO)_4Ag^+$ is evident from the ^1H NMR data. An averaged chemical shift and coupling constant were observed when excess ADPO was added to a CD_2Cl_2 solution of $[(ADPO)_4Ag]^+SbF_6^-$. However, the downfield shift in the ^1H NMR for ring protons is consistent with the planar, oxidized form of the ligand backbone. The increase in $^3J_{PH}$ (9.6→14.3 Hz) is consistent with trends observed for increased phosphorus coordination number is smaller than in previous examples (~26 Hz).[3,6-8] The ^{15}N NMR chemical shift (δ -124.5, $^1J_{PN}$ = 64.4 Hz) is close to uncomplexed ADPO (δ -126.3, $^1J_{PN}$ = 80.0 Hz). The reduction of P-N coupling constant follows the expected trend.[5] The ^{31}P NMR spectrum consists of a broad singlet at δ 166 ppm. The absence of Ag-P coupling down to -95 °C in CD_2Cl_2 reflects the high lability of ADPO ligands. The NMR data suggest that the ligand exchange rate in $[(ADPO)_4Ag]^+SbF_6^-$ is even faster than the rates observed for $Ag[P(C_6H_4CH_3)_3]_4^+$ or $Ag[P(OC_2H_5)_3]_4^+$.[11]

(12) ADPO (500 mg, 2.07 mmol) was dissolved in CH_2Cl_2 (15 mL) and solid $[Ag(NCCH_3)_4]^+SbF_6^-$ (262 mg, 0.517 mmol) was added at room temperature. The resulting yellow-green solution was stirred for 15 min and the volatiles were removed under vacuum. The residue was extracted into CH_2Cl_2, filtered through Celite, and concentrated under reduced pressure. The addition of hexane followed by cooling to -25 °C gave yellow crystals of $[(ADPO)_4Ag]^+SbF_6^-$ (453 mg) in 67% yield, mp 173-174 °C dec. NMR data in CD_2Cl_2: ^1H δ 1.24 (s, 18 H), 7.70 (d, $^3J_{PH}$ = 14.4 Hz, 2 H); $^{13}C\{^1H\}$ δ 27.9 (CH_3), 34.5 ($C(CH_3)_3$), 113.3 (d, J_{PC} = 2.8 Hz, NC), 171.6 (CO); ^{31}P δ 166; ^{15}N δ -124.5 (d, $^1J_{PN}$ = 64.4 Hz) (reference $NH_4{}^{15}NO_3$). Anal. ($C_{48}H_{80}AgF_6N_4O_8P_4Sb$): C, H, N.

(13) Crystal data for $[(ADPO)_4Ag]^+SbF_6^-$ at 203 K with Mo Kα radiation: a = 1619.2 (2) Å, c = 2385.6 (2) pm, tetragonal, $P4/ncc$, Z = 4, 1219 unique reflections with $I > 3\sigma(I)$. The final R factors were R = 0.028, R_w = 0.026. The largest residual density in the final difference Fourier map was 0.03 e/Å^3. Further details of the crystal structure are available in the supplementary material.

(14) Pelizzi, C.; Pelizzi, G.; Tarasconi, P. *J. Organomet. Chem.* **1984**, *277*, 29.

(15) Engelhardt, L. M.; Patawatchai, C.; White, A. H.; Healy, P. C. *J. Chem. Soc., Dalton* **1985**, 125.

(16) Barron, P. F.; Dyason, J. C.; Healy, P. C.; Engelhardt, L. M.; Skelton, B. W.; White, A. H. *J. Chem. Soc., Dalton* **1986**, 1965.

(17) Culley, S. A.; Arduengo, A. J., III *J. Am. Chem. Soc.* **1984**, *106*, 1164.

(18) This drawing was made with the KANVAS computer graphics program. This program is based on the program SCHAKAL by E. Keller (Kristallographisches Institute der Universitat Freiburg, FRG), which was modified by A. J. Arduengo, III (E. I. du Pont de Nemours & Co., Wilmington, DE), to produce the back and shadowed planes. The planes bear a 50-pm grid and the lighting source is at infinity so that shadow size is meaningful.

Supplementary Material Available: A complete description of the X-ray crystallographic structure determination on $[(ADPO)_4Ag]^+SbF_6^-$ including experimental procedures, tables of data, and ORTEP structure drawing (7 pages). Ordering information is given on any current masthead page.

A Novel Iron-Sulfur Center in Nitrile Hydratase from *Brevibacterium* sp.[1]

Mark J. Nelson,*,†,[2a] Haiyong Jin,[2a] Ivan M. Turner, Jr.,[2a] Geoffrey Grove,[2b] Robert C. Scarrow,*,[2b] Bridget A. Brennan,[2c] and Lawrence Que, Jr.*,[2c]

Central Research and Development Department E.I. du Pont de Nemours and Co. Wilmington, Delaware 19880-0328 Department of Chemistry, Haverford College Haverford, Pennsylvania 19041 Department of Chemistry, University of Minnesota Minneapolis, Minnesota 55455

Received June 12, 1991

We report that nitrile hydratase from *Brevibacterium* sp. contains a ferric ion in a biologically novel coordination environment. Nitrile hydratases are bacterial enzymes that catalyze the hydration of nitriles to amides.[3] The best characterized is from *Brevibacterium* sp., strain R312, and is probably an $\alpha_2\beta_2$ tetramer of 94 000 Da.[4,5] The EPR spectrum of this protein (g_1 = 2.27, g_2 = 2.12, g_3 = 1.97) is consistent with a rhombically distorted octahedral, low-spin ferric complex.[6,7] We present resonance Raman and EXAFS spectra that suggest that the iron exists in a ligand field of sulfur and nitrogen or oxygen donor atoms.

The iron k-edge X-ray absorption spectrum[8] (Figure 1a) of nitrile hydratase[9] shows a shoulder at 7116 eV[10] associated with sulfur coordination.[11] The shoulder at 7112 eV, assigned to the

† Please address correspondence to Mark J. Nelson at DuPont.

(1) Contribution No. 5891 from the Central Research and Development Department, E.I. du Pont de Nemours & Co.

(2) (a) E.I. du Pont de Nemours & Co. (b) Haverford College. (c) University of Minnesota.

(3) Nagasawa, T.; Yamada, H. *Trends Biotechnol.* **1989**, *7*, 153-158.

(4) Nagasawa, T.; Ryuno, K.; Yamada, H. *Biochem. Biophys. Res. Commun.* **1986**, *139*, 1305-1312. The molecular weight is estimated from the primary sequences of the subunits ($\alpha \approx 23\,000$; $\beta \approx 23\,500$). Ikehata, O.; Nishiyama, M.; Horinouchi, S.; Beppu, T. *Eur. J. Biochem.* **1989**, *181*, 563-570.

(5) This organism is probably identical with *Rhodococcus* sp., strain N-774. Mayaux, J.-F.; Cerbelaud, E.; Soubrier, F.; Faucher, D.; Petrê, D. *J. Bacteriol.* **1990**, *172*, 6764-6773.

(6) Sugiura, Y.; Kuwahara, J.; Nagasawa, T.; Yamada, H. *J. Am. Chem. Soc.* **1987**, *109*, 5848-5850.

(7) Jin, H.; Nelson, M. J., unpublished.

(8) X-ray fluorescence excitation profiles were obtained by using Canberra 13-element Ge detectors. Samples were frozen in aluminum holders and held near 77 K on a Janis cryostat. The fluorescence signal was converted to EXAFS as described: Scarrow, R. C.; Maroney, M. J.; Palmer, S. M.; Que, L. Jr.; Row, A. L.; Salowe, S. P.; Stubbe, J. *J. Am. Chem. Soc.* **1987**, *109*, 7857-7864.

(9) The enzyme was purified from an amidase-deficient mutant of *Brevibacterium* sp., strain R312, according to a modification of the published procedure.[4] The enzyme solutions used had specific activities ranging from 400 to 600 μmol methacrylonitrile hydrated min^{-1} mg^{-1}, which corresponds to 900-1200 units/mg as measured by hydration of propionitrile.[4] Our preparations contain approximately 1.7 equiv of iron/protein; EPR integrations routinely show 1 ± 0.1 spin/iron. Samples were prepared in 0.01 M HEPES buffer, pH 7.8 (at 4 C), containing 40 mM sodium butyrate as a stabilizing agent.[4]

(10) The X-ray energy (E) was calibrated to the 7113.0-eV preedge peak in an in-line sample of $[Et_4N]_2[FeCl_4]$.

(11) Roe, A. L.; Schneider, D. J.; Mayer, R. J.; Pyrz, J. W.; Widom, J.; Que, L., Jr. *J. Am. Chem. Soc.* **1984**, *106*, 1676-1681.

0002-7863/91/1513-7072$02.50/0 © 1991 American Chemical Society

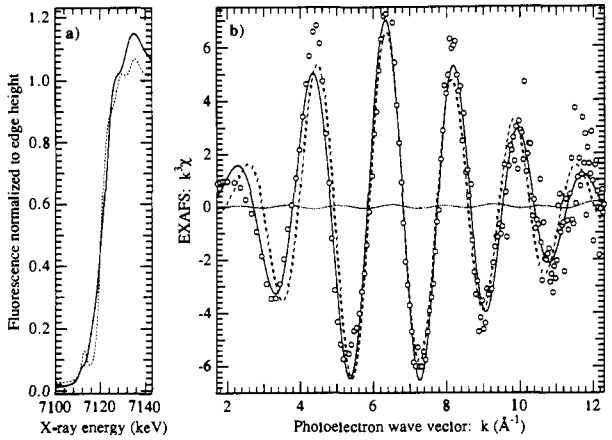

Figure 1. (a) Iron k-edge spectra of nitrile hydratase (—) and $[Et_4N]FeCl_4$ (---), normalized to give an edge height of 1.[10] (b) The EXAFS spectrum of nitrile hydratase before (OOO) and after (—) Fourier filtering (k = 1.7–12.3 Å^{-1}; r' = 1.1–2.3 Å). The best two-shell fit (see text) is indistinguishable from the Fourier filtered data [rms ($\chi-\chi_{calcd}$ = 0.05]; the difference is shown (···). Also shown is the best single-shell fit (---).

1s to 3d transition, has an area of approximately 0.08 eV,[12] much smaller than that observed for rubredoxin (tetrahedral FeS_4),[13] but in the range found for six-coordinate ferric complexes.[11] The best single-shell least-squares fit of the EXAFS data[14,15] (Figure 1b) assumes sulfur scatterers (five at 2.20 Å) rather than nitrogen or oxygen. However, a much better fit was obtained with a two-shell model with 2.5 oxygen or nitrogen scatterers at 1.98 Å and 2.5 sulfur scatterers at 2.21 Å. On the basis of experience with model compounds and refinements employing alternate weighting schemes,[15] we conservatively estimate the accuracy of n to be ±1 and that of r to be ±0.03 Å.[14] The Fe–S bond length is consistent with structurally characterized low-spin ferric thiolate complexes: for example, bis(2-(((2-aminoethyl)imino)methyl)-benzenethiolato)iron(III) has Fe–S bond lengths of 2.21 Å[16] and tris(1,1,1-trifluoro-4-phenyl-4-mercaptobut-3-en-2-onato)iron(III) has Fe–S bond lengths of 2.247, 2.217, and 2.254 Å.[17]

Nitrile hydratase shows an electronic transition at 710 nm ($\epsilon \sim 1100$ M^{-1} cm^{-1}).[4,7] The resonance Raman spectrum obtained with 640-nm excitation (Figure 2) has peaks at 348, 378, 412, 452, and 756 cm^{-1}. Notably absent are peaks in the 1100–1600-cm^{-1} region that would support[18] the suggestion of tyrosine coordinated to the metal ion.[19] The low-frequency features are higher in energy than those found in spectra of tetrahedral high-spin Fe–S centers like rubredoxin[20] and ferredoxins,[21] but, with respect to energy, multiplicity, and intensity,[22] resemble those

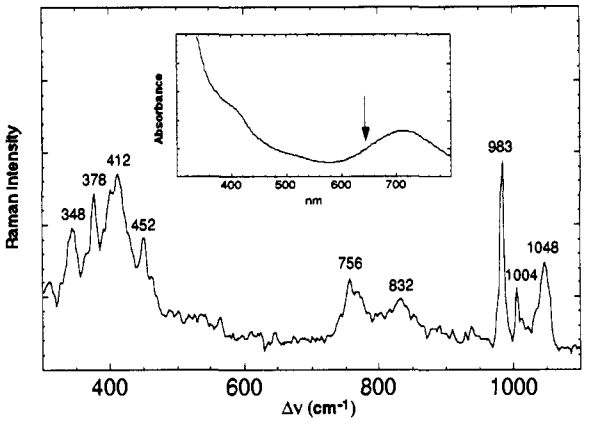

Figure 2. Resonance Raman spectrum of nitrile hydratase. Samples (100 mg/mL) were prepared in 0.01 M HEPES buffer, pH 7.8 (4 °C), containing 40 mM sodium butyrate, and run at 4 °C. The 983- and 1004-cm^{-1} peaks arise from SO_4^{2-}, an internal standard, and phenylalanine in the protein, respectively. All other peaks above 800 cm^{-1} were also found in the buffer.

found for azurin, a bacterial electron-transfer protein of approximately 15 000 Da that contains a blue (type I) copper site. In azurin these characteristics are attributed to vibrations of the relatively strong metal–sulfur bond with coupling to cysteine deformations. We would expect the strong metal–sulfur bond in the low-spin ferric center in nitrile hydratase to give rise to a similar pattern. These features support our assignment of sulfur ligation to the iron and suggest that the 710-nm absorption is a transition with cysteinate-to-iron charge-transfer character. Three of the five cysteines in this enzyme are present in a Cys-X-Y-Cys-Z-Cys motif at residues 110–115 of the α chain,[4,5] which we tentatively assign to the metal binding site by analogy to the well-known Cys-X-Y-Cys sequences that supply cysteine ligands to the iron sites of rubredoxins.[23]

To our knowledge, this is the first reported example of a protein-bound six-coordinate mononuclear non-heme iron with a mixed sulfur and nitrogen or oxygen coordination sphere. There are well-characterized examples of hydratase/dehydratase enzymes that contain iron–sulfur units analogous to those found in both four-iron and two-iron ferredoxins.[24] With nitrile hydratase, this analogy may be extended to the single-iron class of iron–sulfur protein.

Acknowledgment. We gratefully acknowledge the assistance of Drs. Stephen P. Cramer, Simon George, and Syed Khalid. X-ray data were collected at beam lines X9a and X19a of the National Synchrotron Light Source, Brookhaven National Laboratory, supported by the U.S. Department of Energy, Division of Materials Science and Chemical Science (DOE Contract No. DE-AC02-76CH00016). Support for the work at Haverford College was provided by a grant from the Howard Hughes Medical Institute through the Undergraduate Biological Sciences Initiative. L.Q., Jr., acknowledges the National Institutes of Health (GM-33162), and B.A.B. acknowledges an NIH predoctoral fellowship (GM-08277).

Supplementary Material Available: Tables of the various fits considered for nitrile hydratase and model compounds (3 pages). Ordering information is given on any current masthead page.

(12) The units (eV) for the area arise from the normalization of the intensity of the edge.

(13) Shulman, R. G.; Eisenberger, P.; Blumberg, W. E.; Stombaugh, N. A. *Proc. Natl. Acad. Sci. U.S.A.* **1975**, *72*, 4003–4007.

(14) EXAFS is modelled assuming shells of n atoms at distances of $r \pm \sigma$ (σ arises from static and vibrational disorder). $\chi_{calcd} = \sum(naB/kr^2)\exp(-2\sigma^2k^2 - 2r/\lambda)\sin(2kr + 2\delta + \phi)$. B and ϕ (scattering atom functions) are from published ab initio calculations (McKale, A. G.; Veal, B. W.; Paulikas, A. P.; Chan, S.-K.; Knapp, G. S. *J. Am. Chem. Soc.* **1988**, *110*, 3763–3768) while δ (for Fe) is based on the following: Teo, B. K.; Lee, P. A. *J. Am. Chem. Soc.* **1979**, *101*, 2815–2832. $k^2 = 2m_e(E - E_0)/\hbar^2$. On the basis of experience with models,[15] the amplitude reduction factor, a, is taken to be 0.4, and E_0 = 7128 eV for Fe^{3+}–O(N) and 7124 eV for Fe^{3+}–S.

(15) Tables of the various fits considered for nitrile hydratase and model compounds are available as supplementary material.

(16) Fallon, G. D.; Gatehouse, B. M. *J. Chem. Soc., Dalton Trans.* **1975**, 1344–1347.

(17) Hoskins, B. F.; Pannan, C. D. *Inorg. Nucl. Chem. Lett.* **1975**, *11*, 409–413.

(18) Que, L., Jr. In *Biological Applications of Raman Spectroscopy*; Spiro, T. G., Ed.; Wiley-Interscience: New York, 1988; Vol. 3, pp 491–521.

(19) Carrano, C. J.; Carrano, M. W.; Sharma, K.; Backes, G.; Sanders-Loehr, J. *Inorg. Chem.* **1990**, *29*, 1865–1870.

(20) Czernuszewicz, R. S.; LeGall, J.; Moura, I.; Spiro, T. G. *Inorg. Chem.* **1986**, *25*, 696–700.

(21) Han, S.; Czernuszewicz, R. S.; Spiro, T. G. *J. Am. Chem. Soc.* **1989**, *111*, 3496–3504. Han, S.; Czernuszewicz, R. S.; Kimura, T.; Adams, M. W. W.; Spiro, T. G. *J. Am. Chem. Soc.* **1989**, *111*, 3504–3511.

(22) Blair, D. F.; Campbell, G. W.; Schoonover, J. R.; Chan, S. I.; Gray, H. B.; Malmström, B. G.; Pecht, I.; Swanson, B. I.; Woodruff, W. H.; Cho, W. K.; English, A. E.; Fry, H. A.; Lum, V.; Norton, K. A. *J. Am. Chem. Soc.* **1985**, *107*, 5755–5766.

(23) Nakamura, A.; Ueyama, N. In *Metal Clusters in Proteins*; Que, L., Jr., Ed.; Advances in Chemistry 372; American Chemical Society: Washington, DC, 1988, pp. 292–301.

(24) Emptage, M. H.; In *Metal Clusters in Proteins*; Que, L., Jr., Ed.; Advances in Chemistry 372; American Chemical Society: Washington, DC, 1988; pp 343–371. Flint, D.; Emptage, M. H. *J. Biol. Chem.* **1988**, *263*, 3558–3564.